Journal of Applied Sciences

ISSN 1812-5654

science alert

ANSInet
an open access publisher
http://ansinet.com

Journal of Applied Sciences 7 (21): 3242-3248, 2007
ISSN 1812-5654

Inhibitory Effect of Thiourea on Corrosion of BSK46 Microalloyed Steel

Yasair Suliman Al-Faiyz
Department of Chemistry, King Faisal University, P.O. Box 1758, Al-Hassa 31982, Saudi Arabia

Abstract: The efficiency of Thiourea (TU) as a corrosion inhibitor of BSK46 microalloy steel in H_2SO_4 solution was investigated. We examined the effect of a variety of TU concentrations at different temperatures on the microstructural behavior of BSK46 microalloy steel. Polarization data indicated that both concentration and temperature strongly influenced inhibitor efficiency. Thermodynamic studies confirmed that inhibitor adsorption followed the Langmuir Adsorption Isotherm model.

Key words: Microalloyed steel, repeated quenching, corrosion inhibition, thiourea, adsorption, Langmuir isotherm

INTRODUCTION

Due to its environmental and economical effects, steel corrosion consider as a major industrial problem that cost hundreds of billions of dollars (Oluwad and Agbaje, 2007). In order to minimize its adverse effects scientists from varies fields have investigated this problem and many prevention methods have been reported (Ghali *et al*., 2007). One of the most effective solutions for this problem is the use of organic compounds as corrosion inhibitors, especially in acidic environments (Bentiss *et al*., 2007; Chaudhary *et al*., 2007; Larabi *et al*., 2007). Several groups of organic compounds exert inhibitory effects on this kind of corrosion in acidic media. Organic compounds that contain both nitrogen and sulphur have excellent corrosion inhibitory activity compared with others compounds that contain only nitrogen or sulphur (Agrawal *et al*., 2007; Amin *et al*., 2007; Ashassi-Sorkhabi *et al*., 2007) (TU) is used as a corrosion inhibitor for mild steel in acidic solutions (Agrawal and Namboodhiri, 1990; Ahmed and Abdel-Hakam, 1989). On the other hand, it has been reported that repeated recrystallization of microalloyed steels leads to further refining of microstructure (Song *et al*., 2006). Less attention, however, has been paid to combination effects of TU and repeated recrystallization of microalloyed steels under heat treatment conditions. Therefore, the aim of this study is to investigate the effects of TU and repeated recrystallization under heat treatment conditions upon the corrosion resistance property of BSK46 microalloy steel and to evaluate this process according to particular corrosion system and to attempted to correlate the metallurgical concept with the corrosion parameters. For this purpose, TU was added to 1 N H_2SO_4 in four concentrations at three different temperatures. Analysis of the experimental data revealed that both concentration and temperature strongly influenced the efficiency of the inhibitor. Thermodynamic studies confirmed that inhibitor adsorption followed the Langmuir Adsorption Isotherm model.

MATERIALS AND METHODS

This study conducted in Chemistry Department, King Faisal University, Saudi Arabia in 2005-2007.

The main materials used for this study were BSK46 grade microalloyed steel composed of: C = 0.12%, Mn = 1.0%, S = 0.025%, P = 0.025%, Si = 10%, Al = 0.02%, Nb = 0.08% and the remainder Fe.

Experimental: For polarization studies, AR grade H_2SO_4 (Merck) was used to prepare the solutions. Double distilled water was used to make a solution of 1N H_2SO_4. Thiourea was purchased from Sigma-Aldrich (Sigma Chemical Co., St. Louis, MO) and was added to 1N H_2SO_4 in a range of concentrations (1×10^{-4} M-1×10^{-2} M).

Electrochemical techniques: a conventional three-electrode assembly with microalloy steel strips as the working electrode, a saturated calomel electrode as the reference electrode and a graphite rod as the counter electrode. The electrochemical cell was cleaned and then washed with distilled water; 500 mL of the electrolyte solution was used in the cell for each individual run for the polarization measurements. Freshly polished electrodes (specimens) were placed into the electrochemical cell and pre-exposed to the test solution to attain a steady state at zero current potential.

Anodic and cathodic corrosion potentials were recorded in volts vs $Cu/CuSO_4$ for various current values of current density in the absence or presence of various concentrations of inhibitor at three different temperatures

(20, 30 and 40°C). For each individual run, the specimen surface was ground and freshly polished, washed, degreased in ethanol and dried in warm air.

Polarization curves: Polarization of the working electrode, whether anode or cathode, was recorded in volts with reference to the half-cell electrode $Cu/CuSO_4$ for various values of current density. This data was used to calculate the galvanostatic E-I curve. Excel software (Microsoft, Redmond, WA), was used to plot over-voltage, E vs applied current (anodic and cathodic). The best straight line through the linear polarization points was calculated and its intersection with the zero current horizontal provided more accurate E_{corr} values (Fig. 1) for a particular case (BSK46 as-received sample at 20°C).

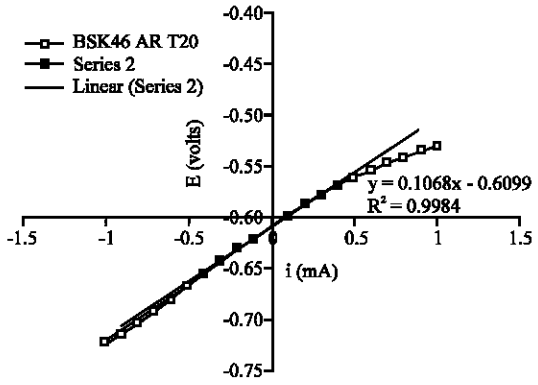

Fig. 1: Linear polarization of BSK46 as-received sample without inhibitor

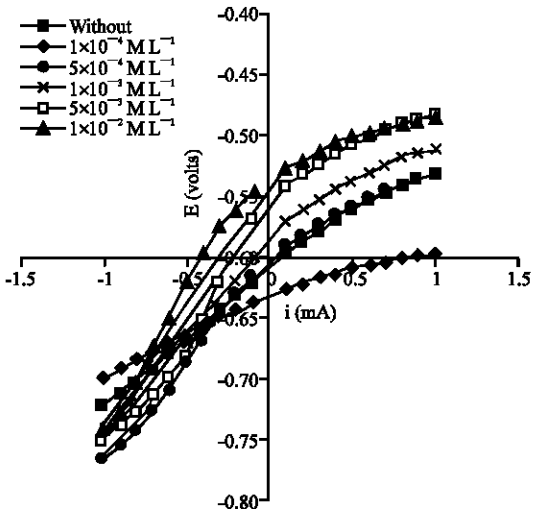

Fig. 2: Linear Polarization of BSK46 as-received sample at 20°C

The results of all the specimens without and with the addition of TU at three different temperatures were confirmed via same techniques some examples (Fig. 2-4).

From the current (i [mA]) and potential (E [volts]) values derived from the polarization experiment, the current density was calculated for all specimens using the area exposed to the electrolyte. Anodic and cathodic polarization (E vs Log I curve) was plotted using a computer and standard software. Using the same software, the best straight line through the Tafel region was plotted and extrapolated. Linear regression equations of the straight lines were obtained. Instead of visual identification of the Tafel region from the polarization curves, a computer method was employed. While selecting the straight lines, a few points were kept in

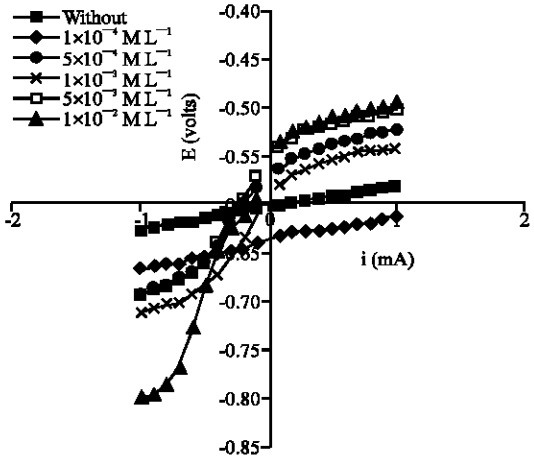

Fig. 3: Linear polarization of BSK46 second-quench sample at 30°C

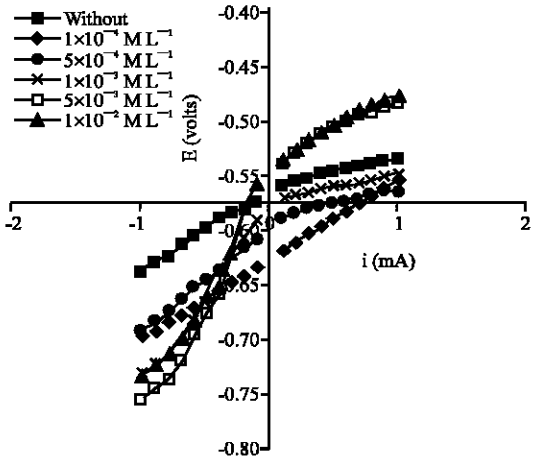

Fig. 4: Linear polarization of BSK46 third-quench sample at 40°C

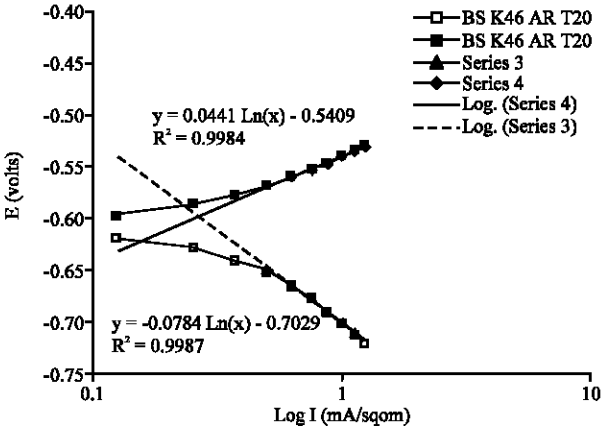

Fig. 5: Polarization diagram of BSK46 as-received sample without inhibitor

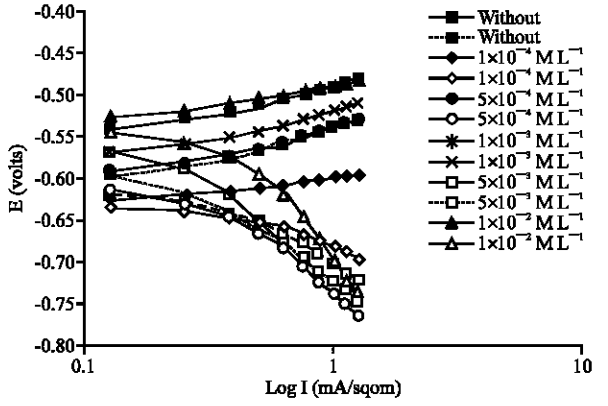

Fig. 6: Polarization Diagram of BSK46 as-received sample at 20°C

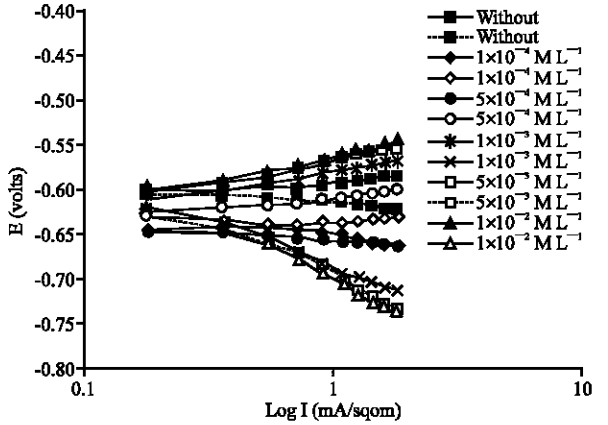

Fig. 7: Polarization Diagram of BSK46 second-quench sample at 30°C

mind; viz., anodic (β_a) and cathodic (β_c) slopes should be close to each other (except for their sign), the interaction of these extrapolations should be close to the experimental E_{corr} and the R^2 values for the straight lines calculated from the experimental data should be very close to 1, as shown in (Fig. 5) for the case BSK46 as-received sample at 20°C.

Polarization diagrams of all specimens without and with the addition of TU were obtained. Some cases are shown in (Fig. 6-8). The calculated E_{corr} and I_{corr} values from the polarization diagram for all the specimens (Table 1, 2).

Table 1: /E_{corr} values of BSK46 (with TU)

Concentrations (mol L^{-1})	Temperature (°C) 20	30	40
As-Received			
1×10^{-4}	-0.631	-0.603	-0.632
5×10^{-4}	-0.604	-0.600	-0.624
1×10^{-3}	-0.584	-0.572	-0.615
5×10^{-3}	-0.552	-0.556	-0.585
1×10^{-2}	-0.536	-0.539	-0.581
First Quench			
1×10^{-4}	-0.628	-0.615	-0.643
5×10^{-4}	-0.590	-0.598	-0.632
1×10^{-3}	-0.569	-0.594	-0.598
5×10^{-3}	-0.545	-0.559	-0.590
1×10^{-2}	-0.540	-0.540	-0.588
Second Quench			
1×10^{-4}	-0.618	-0.648	-0.654
5×10^{-4}	-0.590	-0.629	-0.632
1×10^{-3}	-0.552	-0.619	-0.592
5×10^{-3}	-0.535	-0.612	-0.583
1×10^{-2}	-0.534	-0.611	-0.576
Third Quench			
1×10^{-4}	-0.604	-0.638	-0.649
5×10^{-4}	-0.585	-0.632	-0.624
1×10^{-3}	-0.558	-0.592	-0.605
5×10^{-3}	-0.538	-0.552	-0.575
1×10^{-2}	-0.535	-0.549	-0.574

Table 2: I_{corr} values of BSK 46 (with TU)

Concentrations (mol L^{-1})	Temperature (°C) 20	30	40
As-Received			
1×10^{-4}	0.261	0.265	0.325
5×10^{-4}	0.240	0.245	0.301
1×10^{-3}	0.180	0.185	0.220
5×10^{-3}	0.165	0.165	0.191
1×10^{-2}	0.160	0.161	0.181
First Quench			
1×10^{-4}	0.290	0.305	0.340
5×10^{-4}	0.261	0.275	0.305
1×10^{-3}	0.220	0.230	0.220
5×10^{-3}	0.180	0.185	0.200
1×10^{-2}	0.175	0.18	0.191
Second Quench			
1×10^{-4}	0.320	0.380	0.384
5×10^{-4}	0.285	0.325	0.330
1×10^{-3}	0.241	0.265	0.271
5×10^{-3}	0.210	0.230	0.235
1×10^{-2}	0.205	0.225	0.226
Third Quench			
1×10^{-4}	0.331	0.380	0.390
5×10^{-4}	0.281	0.320	0.330
1×10^{-3}	0.220	0.250	0.260
5×10^{-3}	0.205	0.220	0.225
1×10^{-2}	0.200	0.215	0.215

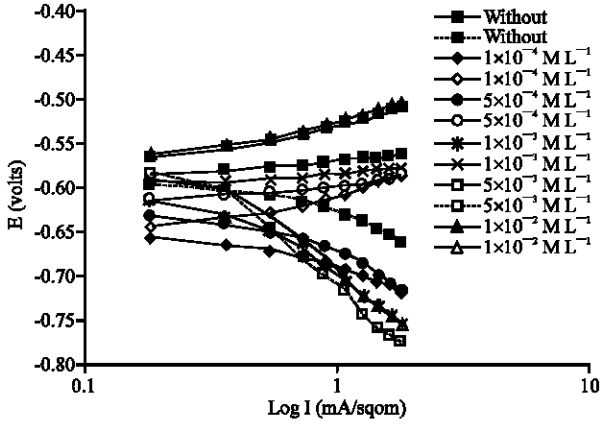

Fig. 8: Polarization diagram of BSK46 third-quench sample at 40°C

RESULTS AND DISCUSSION

The polarization diagrams show that at every temperature, all the polarization curves shifted towards lower values of I_{corr} in proportion to the inhibitor concentration added. Also, E_{corr} values of BSK46 in inhibitor-containing solution shifted towards more noble values with increased TU inhibitor concentration. The addition of TU did not affect the cathodic Tafel region, thought to be a result of extrapolating the cathodic Tafel region. At high temperature and high TU concentrations, the limiting current density region overshadows the Tafel region, possibly because TU adsorption increases as a result of decreased hydrogen ion mobility to the cathode. The cathodic reaction is therefore highly retarded and the cathodic Tafel slope could not be drawn. The anodic Tafel slope, however, is clear and nearly the same for all concentrations. A straight line for the anodic Tafel region was drawn and its intersection with the horizontal line through E_{corr} gives the I_{corr} for all concentrations. The E_{corr} values (Table 1) indicate that corrosion potential shifted to more noble values due to the addition of TU and only the anodic process was affected by this addition (Fig. 9). This observation is consist with other finding that in mild steel corrosion TU and its derivative effect the anodic process only (Shetty *et al*., 2007).

I_0 = corrosion rate of the uninhibited system (i.e., without inhibitor) and I is the corrosion rate of the inhibited system (i.e., with inhibitor). First, θ values were calculated from I_0 and I values and then percent inhibitor efficiency was calculated. The values of inhibitor efficiency (%) (Table 3).

In All repeated quench sample and at any given temperature, corrosion rates (I_{corr}) decreased with an increase in< TU. This was correlated with the increasing degree of surface coverage due to repeated recrystallization. Corrosion rate as function of TU concentration (Fig. 10).

Table 3: Inhibitor Efficiency (%) of BSK46 Microalloyed Steels

Concentrations (Mol L^{-1})	Temperature (°C) 20	30	40
As-Received			
1×10^{-4}	5.45	7.02	7.14
5×10^{-4}	12.72	14.03	14.28
1×10^{-3}	34.54	35.08	37.14
5×10^{-3}	40.00	42.10	45.71
1×10^{-2}	41.82	43.86	48.57
First Quench			
1×10^{-4}	6.45	7.58	8.11
5×10^{-4}	16.13	16.67	17.56
1×10^{-3}	29.03	30.30	40.54
5×10^{-3}	41.93	43.94	45.95
1×10^{-2}	43.55	45.45	48.65
Second Quench			
1×10^{-4}	5.88	7.32	8.33
5×10^{-4}	16.17	20.73	21.43
1×10^{-3}	29.41	35.36	34.15
5×10^{-3}	38.23	43.90	44.05
1×10^{-2}	39.71	45.12	46.43
Third Quench			
1×10^{-4}	5.71	7.32	9.30
5×10^{-4}	20.00	21.95	23.26
1×10^{-3}	37.14	39.02	39.53
5×10^{-3}	41.42	46.34	47.67
1×10^{-2}	42.86	47.56	50.00

The inhibitor efficiency of BSK46 for as-received samples increased with higher TU concentrations for all three temperatures (Table 3). The degree of surface coverage increases with an increased in temperature for the as-received microalloyed steel and there was an appreciable degree of protection (even at very low inhibitor concentrations). This finding strongly supports the idea that the TU inhibits the corrosion process through surface adsorption.

The trends for the E_{corr}, I_{corr} and inhibitor efficiency values were the same for samples quenched once, twice and three times (Table 1-3) but they reached maximum values for the samples quenched three times. The reason behind that is believe to be the increases of the grain size of ferritic microalloyed steel due to repeated recrystallization. Also, the inhibitor efficiency increased with an increase in the TU concentration, but it reached a maximum at 1×10^{-2} M L^{-1} for all treatments.

Polarization properties: The polarization properties of the repeatedly recrystallized samples were the same as those of the as-received samples of each grade. All the polarization curves shifted towards lower I_{corr} values in proportion to the TU concentration. E_{corr} values in the solution containing inhibitor shifted towards more noble values as the inhibitor concentration increased (Table 2). For samples quenched three times, the E_{corr}, for all samples

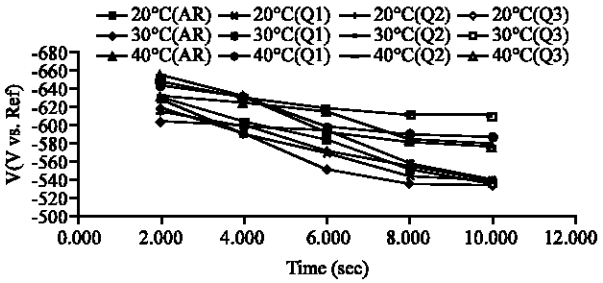

Fig. 9: Potential vs. time plot

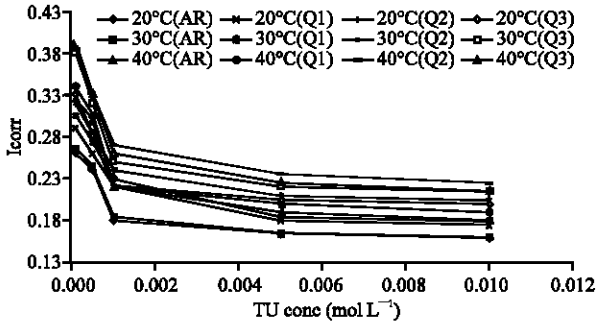

Fig. 10: Corrosion rate as a function of TU concentration

with and without TU shifted to more noble values due to the repeated recrystallization, indicating that the addition of TU affects mainly the anodic process. These same results were also observed for the samples quenched twice. The I_{corr} values of the samples quenched three times in the uninhibited solution were 0.35, 0.42 and 0.43 and in the samples quenched three times with 1×10^{-2} M L^{-1} TU solution were 0.20, 0.215 and 0.215 at 20, 30 and 40°, respectively (Table 2). Thus, due to an increase in TU concentration, the I_{corr} values decreased for quenched steel at all three temperatures. The same results were observed for the samples recrystallized twice.

Inhibitor efficiency: Inhibitor efficiency or the degree of surface coverage increases with an increased increase in temperature and in TU concentration for repeatedly recrystallized microalloyed steel (Table 3). These results also indicate that there was no change in the inhibitor efficiency of TU due to repeated quenching. The inhibitor efficiency values for the highest concentration of TU were nearly the same in as-received and repeatedly recrystallized samples. Thus, the use of TU with repeated recrystallization of the BSK46 microalloyed steels has a little effect on grain refinement.

Adsorption isotherm: The Surface Coverage (θ) values were tested graphically for fitting to a suitable adsorption isotherm. The different types of adsorption isotherm equations that might govern the adsorption processes are:

$f(\theta) = \{\theta/(1-\theta)\}\times\{\theta + n(1-\theta)^{n-1}/n^n\}$ as per the Bockris-Swinkel model, $f(9) = 9/\exp(n-1)(1-9)''$ as per the Flory-Huggins model (Abiola, 2005) or $\theta = K.C_{inh}/(1+K.C_{inh})$ and $C_{inh}/\theta = C_{inh}+1/K$ as per the Langmuir model (Alberty and Silbey, 1998).

In the above equations (n) is an integer and (C_{inh}) represents inhibitor concentration. The data were tested in each model systematically, but failed to fit either the Bockris-Swinkel isotherm model or the Flory-Huggins isotherm model. The plots of C_{inh}/θ vs. C_{inh} yield (Fig. 11) a straight line for the as-received and quenched samples at three different temperatures, which clearly demonstrates that this adsorption process followed the Langmuir Adsorption Isotherm model and is consistent with other findings that the inhibition of TU-derived inhibition of corrosion in mild steel obeys the Langmuir Adsorption Isotherm model (Azim *et al*., 1998).

Mechanism of inhibition: The free energy of adsorption ($\Delta G°ads$) at different temperatures was calculated from the Langmuir adsorption isotherm curve C_{inh}/θ vs. C_{inh}. The intercept (1/K) of the straight line, where K represents the adsorption coefficient, which is temperature dependent and related to Gibb's Free Energy ($\Delta G°ads$) and hence to the enthalpy change ($\Delta H°ads$) of the process:

$$K = \exp(\Delta G°ads/RT) \text{ and}$$
$$\Delta G°ads = \Delta H°ads - T\Delta S \text{ ads.}$$

Table 4 shows the-$\Delta G°ads$ values of as-received BSK46 samples at 20, 30 and 40°C for the first, second and third quenches. The free energy of adsorption had negative values for all the as-received and quenched steels. An increase in temperature increased the free energy change (-$\Delta G°ads$) values. The low and negative values of $\Delta G°ads$ indicate the spontaneous adsorption of inhibitors on the metal surface, as reported for mild steel (Ajmal *et al*., 2000). The $\Delta H°ads$ and $\Delta S°ads$ of the BSK46 microalloyed steel are (Table 5). The enthalpy change of the adsorption process was negative ($\Delta H°$ ads< 0), i.e., adsorption is an exothermic reaction as reported by others for mild steel (Divakar *et al*., 2007).

At every temperature examined, the polarization curves shifted towards lower I_{corr} values in proportion to the TU concentration (Table 2). E_{corr} values in the TU solution shifted towards more noble values with an increase in the TU concentration (Table 1). The degree of surface coverage (i.e., inhibitor efficiency) increased with the increase in temperature for as-received microalloyed

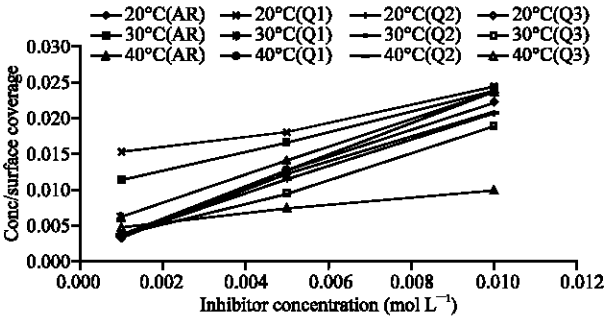

Fig. 11: Langmuir's isotherm adsorption on plots of for the all samples

Table 4: Free energy (-ΔG° KJ/Mole) values of BSK46

Temp. (°C)	AR	Q1	Q2	Q3
20	-15.536	-15.840	-16.008	-16.596
30	-16.381	-16.554	-17.162	-17.403
40	-16.922	-17.502	-17.728	-18.250

Table 5: Enthalpy and entropy changes in BSK46 microalloyed steel

ΔH°ads	ΔS°ads
-14.3	0.0693
-14.139	0.0832
-14.3	0.0861
-14.934	0.0828

steel (Table 3). The E_{corr}, I_{corr} and inhibitor efficiency value trends were the same for the first, second and third quench samples in each case, but the values reached maximum for the third quench sample (Table 3).

The inhibitor efficiency increased with an increase in the TU concentration. The polarization properties of the repeatedly recrystallized samples were the same as that of the as-received samples of each grade. In the repeatedly recrystallized samples, the corrosion potential shifted to more noble values. This finding indicates that the addition of a TU inhibitor affects mainly the anodic process. Therefore, an increase in TU concentration decreased the I_{corr} corrosion rate for recrystallized steel at all three temperatures examined.

The inhibitor efficiency and the degree of surface coverage increased with an increase in temperature and in TU concentration for repeatedly recrystallized microalloyed steel.

The adsorption process of TU in 1(N) H_2SO_4 solution on the microalloyed steel surface follows the Langmuir Adsorption Isotherm model.

The free energy of adsorption shows negative values for all the as-received and quenched steel samples.

As the temperature increases, the free energy change (-ΔG°ads) increases as well. The enthalpy change of the adsorption process is negative (ΔH°ads< 0) (i.e., adsorption is an exothermic reaction).

CONCLUSIONS

The addition of a TU inhibitor affects mainly the anodic process and the efficiency of this compound as an inhibitor increases as the concentration and temperature increase. An increase in the TU concentration decreased the corrosion rate in repeatedly quenched microalloyed steel at all three temperatures. Although the trend of the efficiency values was the same for the first, second and third quenched samples, these values reached a maximum for the third quench sample. This inhibition process is an exothermic reaction and follows the Langmuir adsorption isotherm model.

ACKNOWLEDGMENT

The author is grateful to the deanship of scientific research of King Faisal University for their financial support.

REFERENCES

Abiola, O.K., 2005. Adsorption of methionine on mild steel. J. Clin. Chem. Soc., 50: 685-690.

Agrawal, R. and T.K.G. Namboodhiri, 1990. The inhibition of sulphuric acid corrosion of 410 stainless steel by thioureas. Corrosion Sci., 30: 23-36.

Agrawal, R.M., V.R. Chourey and S.L. Garg, 2007. Studies in protective coatings of metals with special reference to organic inhibitors mixed with polyurethane. Asian J. Chem., 19: 1170-1176.

Ahmed, A.I. and S. Abdel-Hakam, 1989. Inhibition of the acid corrosion of zinc by some thiourea derivatives. Anti-Corrosion Methods Mat., 36: 4-7.

Ajmal, M., D. Jamal and M.A. Quraishi, 2000. Fatty acid oxadiazoles as acid corrosion inhibitors for mild steel. Anti-Corrosion Methods and Materials, 47: 77-82.

Alberty, R.A. and R. Silbey, 1998. Physical Chemistry. 2nd Edn. Wiley and Sons, New York.

Amin, M.A., S.S. Abd El-Rehim, E.E.F. El-Sherbini and R.S. Bayoumi, 2007. The inhibition of low carbon steel corrosion in hydrochloric acid solutions by succinic acid. Part 1. weight loss, polarization, EIS, PZC, EDX and SEM studies. Electrochim. Acta, 52: 3588-3600.

Ashassi-Sorkhabi, H., T.A. Aliyev, S. Nasiri and R. Zareipoor, 2007. Inhibiting effects of some synthesized organic compound on the corrosion of st-3 in 0.1N H_2SO_4 solution. Electrochimica Acta, 52: 5238-5241.

Azim, S.S., S. Muralidharan, S. Venkatakrishna Iyer, Muralidharan and T.B. Vasudevan, 1998. Synergistic influence of iodide ions on inhibition of corrosion of mild steel in H_2SO_4 by N-phenyl Thiourea. Br. Corrosion J., 33: 297-301.

Bentiss, F., M. Bouanis, B. Mernari, M. Traisnel, H. Vezin and M Lagren´ee, 2007. Understanding the adsorption of 4H-1,2,4-triazole derivatives on mild steel surface in molar hydrochloric acid. Applied Surface Sci., 253: 3696-3704.

Chaudhary, R.S., D.K. Tyagi, M. Rani and A. Kumar, 2007. Corrosion inhibition of mild steel by ethanolamides in hydrochloric acid. J. Sci. Ind. Res., 66: 47-51.

Ghali, E., S. Vedula Sastri and M. Elboujdaini, 2007. Corrosion Prevention and Protection: Practical Solutions Wiley and Sons, New York.

Larabi, L., O. Benali and Y. Harek, 2007. Corrosion inhibition of cold rolled steel in 1 M $HClO_4$ solutions by N-naphtyl N'-phenylthiourea. Mat. Lett., 61: 3287-3291.

Oluwad, G.O. and O. Agbaje, 2007. Corrosion of steel in steel reinforced concrete in cassave juice. J. Applied Sci. (In Press).

Shetty, S.D., Prakash Shetty and H.V. Sudhaker Nayak, 2007. The inhibition action of N-furfuryl-N-phenyl thiourea on the corrosion of mild steel in hydrochloric acid medium. Mat. Lett., 61: 2347-2349.

Song, R., D. Ponge, D. Raabe, J.G. Speer and D.K. Matlock, 2006. Overview of processing, microstructure and mechanical properties of ultrafine grained bcc steels. Mat. Sci. Eng. A., 441: 1-17.